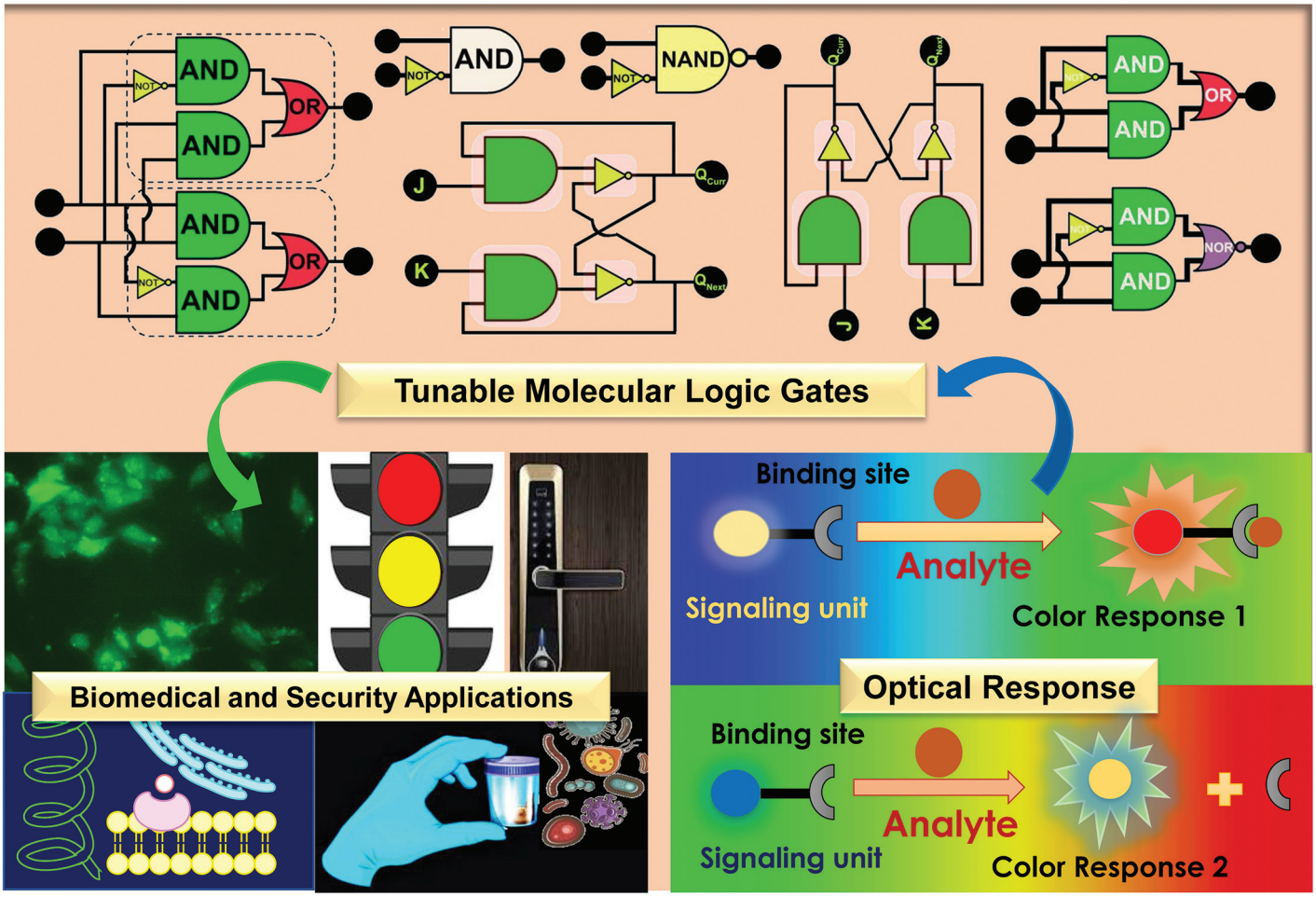

Showcasing research from Dr. Nilanjan Dey's laboratory, Department of Chemistry, Birla Institute of Technology and Science Pilani, Hyderabad, India.

Differential response for multiple ions: smart probe to construct optically tunable molecular logic systems

In this work, we have designed numerous trivial (OR, NOR) as well as non-trivial (INHIBIT, IMPLICATION, COMPLEMENT, TRANSFER, NOT-TRANSFER) logic gates based on differential optical responses of a single molecular probe towards various heavy metal pollutants and anions, such as Cu^{2+}, Hg^{2+}, CN^- and I^-. In general, Dr. Dey's laboratory focuses on developing optical probes for biomolecules, investigating photochemical properties in confined media, designing vehicles for drug and gene delivery, developing responsive soft materials for biomedical applications, agriculture, sustainable chemistry, etc.

As featured in:

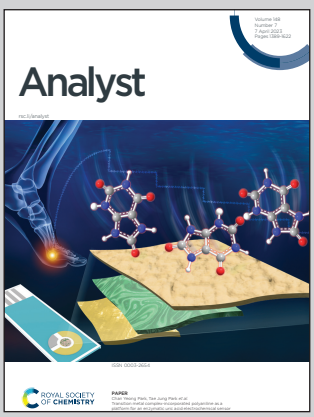

See Nilanjan Dey *et al.*, *Analyst*, 2023, **148**, 1460.

ROYAL SOCIETY OF CHEMISTRY

rsc.li/analyst

Registered charity number: 207890

Analyst

ROYAL SOCIETY OF CHEMISTRY

PAPER

View Article Online
View Journal | View Issue

Cite this: *Analyst*, 2023, **148**, 1460

Differential response for multiple ions: a smart probe to construct optically tunable molecular logic systems†

Monaj Karar,‡[a] Rikitha S. Fernandes‡[b] and Nilanjan Dey *[b]

Received 28th November 2022,
Accepted 25th January 2023

DOI: 10.1039/d2an01945k

rsc.li/analyst

A rhodamine-based optical probe has been designed through a one-pot synthetic protocol involving phenanthroline as a binding motif. The compound showed a bright pink coloration specifically upon the addition of Cu^{2+} and Hg^{2+} ions. However, the appearance of bright red fluorescence was observed only in the presence of Hg^{2+}. Considering both, we can detect and discriminate these two ions even at ppb level concentration. Furthermore, these *in situ* generated metal complexes were utilized for the selective recognition of CN^- and I^- ions. Pre-coated TLC plates were developed for rapid on-site detection of these toxic ions even in remote places. Finally, on a single molecular probe based on differential opto-chemical interactions with different ions (Cu^{2+}, Hg^{2+}, CN^- and I^-), we were able to design numerous trivial (OR, NOR) and non-trivial (INHIBIT, IMPLICATION, COMPLEMENT, TRANSFER, NOT-TRANSFER) logic gates. Most fascinatingly, we can switch the logic response from one type to another by simply tuning only the optical output channel.

1. Introduction

Although the involvement of transition metal ions in regulating different physiological processes are well documented, their excess intake can cause serious health problems, even leading to death. Despite being essential for optimal activities of various metalloenzymes, including superoxide dismutase, cytochrome c oxidase, and tyrosinase,[1] an excess consumption of copper may cause gastrointestinal disorders and several neurodegenerative diseases, such as Wilson's disease and Alzheimer's disease.[2] On the other hand, mercury is known for its extensive utilization in various industries but is highly carcinogenic in nature. Among anions, despite its notorious tendency to bind with the enzyme cytochrome oxidase, cyanide has been continued to be used in gold or silver extraction and in the production of organic chemicals and polymers.[3] Similarly, iodide is considered to be the most essential micronutrient responsible for normal functioning of the thyroid gland. Thus, both iodide deficiency and its excessive intake can lead to several diseases related to malfunctioning of the thyroid gland.[4] Therefore, the United States Environmental Protection Agency (EPA) has listed many transition metal ions and toxic anions, such as chromium, cobalt, copper, mercury, cadmium, and cyanide, as "priority pollutants".

The employment of small molecule-based optical sensors in the recognition of these ionic analytes has gained immense popularity in recent years for their simple execution protocols, high sensitivity, and cost-effectiveness. Nowadays, optical probes are generally designed with binding sites covalently attached to different signaling moieties, such as pyrene, BODIPY, naphthalene, cyanine, and rhodamine.[5] Among them, rhodamine-based probes have received special attention due to the simple synthetic protocols and stimuli-responsive photophysical behavior. After its first introduction by Czarnik *et al.* in 1997, numerous reports have appeared in literature for the detection of a wide range of analytes including metal ions, anions, amino acids and reactive oxygen species.[6] However, optical probes for the detection of multiple ionic analytes are indeed very rare in literature, even by employing rhodamine as the signaling moiety.[7] Sometimes, it has also been observed that multiple ions can interact with the probe molecule in the same fashion due to their similar complexation ability, producing identical signals.[8] Although these kinds of sensors can report the presence of multiple ions, proper identification of interacting analytes is difficult due to indistinguishable optical responses. The discrimination of multiple ions can be

[a]*Department of Humanities and Science, MLR Institute of Technology, Hyderabad, Telangana 500 043, India*
[b]*Department of Chemistry, Birla Institute of Technology and Science Pilani, Hyderabad, Telangana 500078, India. E-mail: nilanjandey.iisc@gmail.com, nilanjan@hyderabad.bits-pilani.ac.in*

†Electronic supplementary information (ESI) available: Additional absorption and emission spectra, time-dependent fluorescence data, FT-IR spectra, ESI-MS analysis, and ^{1}H NMR titration data. The characterizations of the probe molecules were also presented. See DOI: https://doi.org/10.1039/d2an01945k

‡Both authors contributed equally to this work.

achieved simultaneously by exploiting the differential reactivity of the analytes towards a particular guest analyte (indicator dye or metal ion) or a 'chemical event'.

Molecular systems that are capable of responding to external perturbations (like cations, anions, other molecules, ion-pairs) with extensive changes in different spectral experiments are important to the design of molecular logic devices.[9–16] Since its emergence in 1992, ground breaking research was made by the scientific community with elementary supramolecular systems to create and develop fundamental logic components and circuits. To realise the futuristic smart molecular devices, such molecular logic components should be the fundamental integral parts. In this aspect, molecular systems developed with synthesized and commercially available molecules are found to be most promising. It was well established that molecular systems or devices can act as several electronic analogues, like switches,[9] wires,[10] diodes[11] as well as logic gates. Following de Silva,[13] who first introduced the concept of molecular computing, enormous efforts have been given by the chemists to design smart functional molecules that can imitate the functions of various fundamental logic gates, such as YES, NOT, AND, OR, NAND IMPLICATION, INHIBIT, and TRANSFER. Moreover, based on functional integration in a single molecule, several high-order functions (such as half-adder/half-subtractor,[17–19] multiplexer/demultiplexer[20–22]) were constructed.

2. Rationalization of the proposed work

Thus, considering the urge to devise single molecular probes for the sensing of multiple analytes, herein, we have designed a new rhodamine-based probe **1** involving a planar phenanthroline moiety as the metal ion binding site. Compound **1** showed colorimetric detection, as well as discrimination of Cu^{2+} and Hg^{2+} ion below ppb level concentration. However, in the presence of all of the metal ions along with Cu^{2+}, **1** showed its strong and selective attraction towards Hg^{2+} only. Furthermore, the *in situ* generated metal complexes (with Cu^{2+} and Hg^{2+}) were utilized as templates for anion recognition. Again, herein, the 'naked-eye' detection of two different anions cyanide and iodide was achieved. Thus, here we could achieve the detection of all four different ionic analytes simultaneously using a single optical probe. The probe was also further employed for quantification of excess metal ion impurities in different natural water sources, such as, tap water, pool water and sea water. Finally, low-cost, portable, paper-discs were developed for the rapid on-field estimation of these hazardous analytes, even in remote villages.

By maintaining the initial state and chemical inputs unaltered, we simultaneously anticipated that we would assume in a line to acquire multifunctional logic operations to apply to the suggested chemosensing system *via* solely modulations in optical parameters. With favoured outsets, we utilised our synthesized new rhodamine-based probe **1** involving the planar phenanthroline moiety (Scheme 1) to layout tunable molecular logic systems. As we put into operation, the absorption spectral adjustments occurred from one channel to another one, and the consummate logic behaviour switching of **1** occurred from one kind to another. In the same preliminary system, **1** may want to be tuned to act as any other set of inter-switchable complementary logic gates with a specific set of inputs. With **1** as a prototype system and a unique set of inputs, the proposed system is quite flexible to create non-trivial logic gates like INHIBIT, IMPLICATION, COMPLEMENT, TRANSFER, and NOT-TRANSFER as well as some trivial logic gates like OR, NOR, and others. It is fascinating to note that the switching of gates inside a couple of pairs basically involved optical output modulations.

3. Experimental section

3.1. Materials and methods

All reagents, starting materials, analytes and solvents were obtained from the best-known local suppliers and used without further purification. The solvents were distilled prior

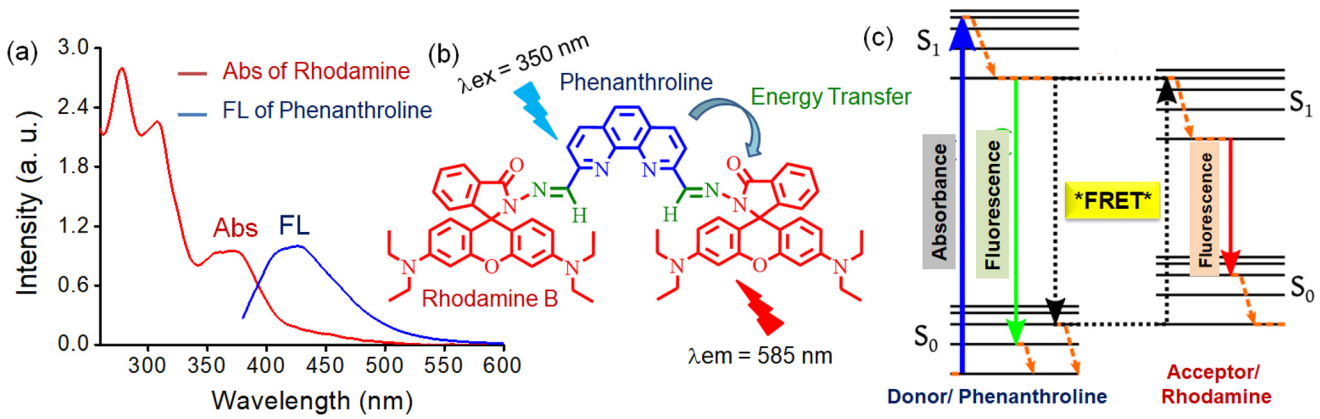

Scheme 1 (a) UV-visible and fluorescence spectra of rhodamine and phenanthroline dyes respectively. (b) Molecular structure **1**. (c) Simple Jablonski diagram focusing on the FRET process.

to use. FT-IR spectra were recorded on a PerkinElmer FT-IR Spectrum BX system, and were reported in wavenumbers (cm^{-1}). ^1H and ^{13}C NMR spectra were recorded on a Bruker-400 Advance NMR spectrometer. Chemical shifts were reported in ppm downfield from the internal standard, tetramethylsilane. Mass spectra were recorded on a Micromass Q-TOF Micro TM spectrometer.

3.2. Sampling procedure of sensing

The sensing studies with metal ions were carried out by adding 10 μL DMSO solution of **1** from a stock solution (1×10^{-3} M) in acetonitrile–water (1 : 1) mixture to make the final volume of 1 mL ([**1**] = 1×10^{-5} M), followed by the addition of a DMSO solution of the metal ions (1 equiv.). In the case of sensing in the buffered medium, a similar procedure has been followed for the sensing in buffered media of different pH values (HCO_2Na/HCl buffer for pH 2, Tris/HCl for pH 7, and $Na_2B_4O_7{\cdot}10H_2O$/NaOH for pH 12). The anion sensing studies were conducted with *in situ* metal complexes (**1**·Cu^{2+} and **1**·Hg^{2+}). For this, the probe with corresponding metal ion (1 equiv.) was incubated in acetonitrile–water (1 : 1) medium for ~2 h prior to the addition of anions (2 equiv.). In all cases, the final concentration of DMSO in the solution did not exceed 1%.

3.3. UV–Vis and fluorescence spectroscopy

The UV–Vis and fluorescence spectroscopy were recorded on a Shimadzu model 2100 spectrometer and Cary Eclipse spectrofluorometer, respectively. The slit-width for the fluorescence experiment was kept at 5 nm (excitation) and 5 nm (emission), and the excitation wavelength was set at 355 nm.

3.4. Fluorescence decay experiment

Fluorescence lifetime values were measured by a time-correlated single photon counting fluorimeter (Horiba Jobin Yvon). The system was excited with 320 nm nano LED of Horiba – Jobin Yvon with a pulse duration of 1.2 ns (slit width of 2/2, λ_{em} is 585 nm). Average fluorescence lifetimes (τ_{av}) for the exponential iterative fitting were calculated from the decay times (τ_i) and the relative amplitudes (a_i) using the following relation,

$$\tau_{av} = (a_1{\tau_1}^2 + a_2{\tau_2}^2 + a_3{\tau_3}^2)/(a_1\tau_1 + a_2\tau_2 + a_3\tau_3)$$

where a_1, a_2 and a_3 are the relative amplitudes and τ_1, τ_2, and τ_3 are the lifetime values, respectively. For data fitting, a DAS6 analysis software version 6.2 was used.

3.5. Preparation of paper discs for sensing

To prepare the compound-coated paper strips, 40 μL of $CHCl_3$–MeOH (1 : 1) solution of **1** (0.02 mM) was drop-cast onto the filter paper using a micropipette. The concentration of **1** in the solution, as well as dipping time, were optimized to obtain photostable test strips with optimal color or fluorescence intensity. The solution was completely absorbed in filter paper within 15 min, and then the filter papers were kept overnight to airdry. Finally, the air-dried paper strips were ready for sensing studies. The stability of the paper strips was evaluated by measuring the fluorescence intensity at intervals of over 15 days.

3.6. Quantification studies

For the quantification of metal ions, the changes in absorbance were recorded at 562 nm. The recovery values (in %) were calculated according to the following equation:

$$\%\text{recovery} = (C_{added} - C_{calculated})/C_{added} \times 100$$

where C_{added} is the actual concentrations of metal ions (Cu^{2+} or Hg^{2+}) spiked into the samples, and $C_{calculated}$ is their calculated values using the standard equation.

3.7. Fluorescence quantum yield

The fluorescence quantum yield was calculated by rhodamine 6G (F = 0.94 in EtOH) as a reference. The quantum yield is calculated using the equation,

$$\Phi_{unk} = \Phi_{std}\ [(I_{unk}/A_{unk})/(I_{std}/A_{std})](\eta_{unk}/\eta_{std})^2$$

where Φ_{unk} and Φ_{std} are the radiative quantum yields of the sample and standard, I_{unk} and I_{std} are the integrated emission intensities of the corrected spectra for the sample and standard, A_{unk} and A_{std} are the absorbances of the sample and standard at the excitation wavelength, and η_{unk} and η_{std} are the indices of refraction of the sample and standard solutions, respectively.

3.8. Analysis of water samples

To evaluate the efficiency of **1** in estimating Hg^{2+} or Cu^{2+} in environmental samples, the performance of the present method was examined by testing tap water, pond water, and seawater samples. The tap water samples were collected from the laboratory. The pond water samples were collected from the local Shameerpet Lake, Telangana, India. The seawater samples were collected from the Bay of Bengal (near Vizag beach). The tap water and pond water samples were subjected to analysis as received. However, the seawater samples were filtered through a 0.22 μm membrane to remove the insoluble dirt particles. The water samples were spiked with different amounts of Cu^{2+} or Hg^{2+} more than 2 h before the analysis.

4. Results and discussion

The compound **1** was designed by the coupling of phenanthroline dialdehyde with rhodamine hydrazone through a carbonyl-nucleophile addition protocol (Scheme S1†). Absorption spectra of **1** showed the presence of multiple maxima at 277 nm ($\varepsilon = 2.42 \times 10^4$), 310 nm ($\varepsilon = 3.20 \times 10^4$) and 375 nm ($\varepsilon = 1.34 \times 10^4$). The bands at 277 nm and 310 nm could be assigned to the π–π* transition, while the n–π* transition resulted in the formation of a peak at 375 nm (Fig. 1a). The presence of an orthogonal spirolactam ring in **1** prevents elec-

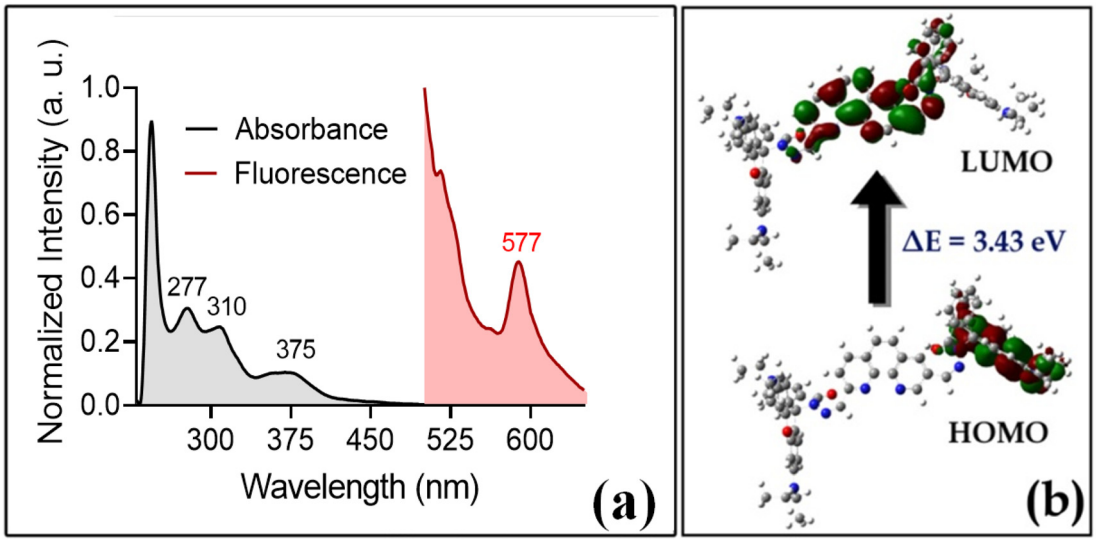

Fig. 1 (a) Normalized absorption and emission spectra of **1** (10 μM, λ_{ex} = 355 nm) in acetonitrile–water (1 : 1) mixture. (b) Frontier Molecular Orbital (FMO) analysis of **1**.

tronic mixing of the electron-rich xanthene moiety with the comparatively electron-deficient phenanthroline site. Therefore, in the free probe, HOMO was found to be largely concentrated on the xanthene fragment, whereas the LUMO was mainly focused on the phenanthroline unit. The higher HOMO–LUMO energy gap (ΔE = 3.43 eV) is reflected from its colorless texture in normal daylight (Fig. 1b).[23] No detectable change in the absorbance value of **1** at 310 nm was noticed when recorded after ~7 days in acetonitrile–water (1 : 1) mixture medium (Fig. S4†). This indicates that the compound is fairly stable under ambient condition, and can be used as a colorimetric probe for target ions.

4.1. Interaction with different metal ions

As the phenanthroline and rhodamine moieties are both known for having metal ion chelating ability at physiological pH, we were interested in exploring the cation sensing property of compound **1** (conjugated adduct of both phenanthroline and rhodamine) at pH 7.4 in a semi-aqueous environment. The addition of Cu^{2+} and Hg^{2+} to the solution of **1** ([**1**] = 10 μM) induced a rapid color change from colorless to bright pink with the appearance of a new absorption band (~560 nm) in the visible region (Fig. 2a). This major red-shift in the n-π* transition band (~560 nm) resulted from the formation of an

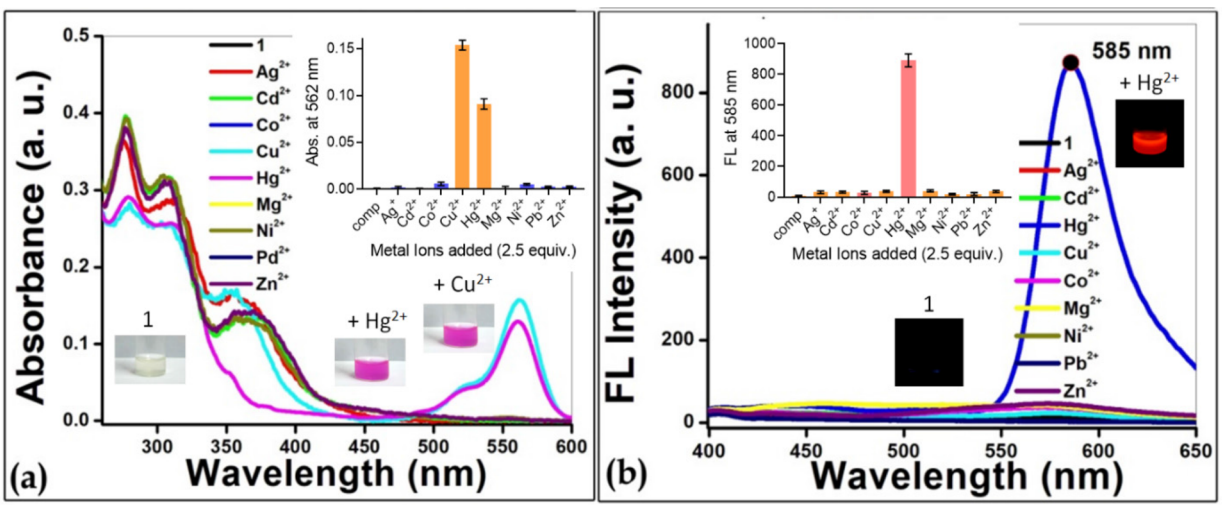

Fig. 2 (a) Absorption spectral changes of **1** in the presence of different cations. Inset: Absorbance bar response at 562 nm for different metal ions. Top: Images of **1** (20 μM) in the presence of different metal ions (1 equiv.) in daylight. (b) Fluorescence spectral changes of **1** in the presence of different cations. Inset: Fluorescence bar response at 585 nm for different metal ions. Top: Images of **1** (10 μM, λ_{ex} = 355 nm) in the presence of different metal ions (1 equiv.) under a long UV lamp.

extended conjugated structure, followed by a reversible spirolactam ring opening process. No spectral change was observed upon the addition of other competing metal ions. Saturation in the optical response was achieved upon the addition of ~2 equiv. of metal ions in both cases (Fig. S5 and S6†). The titration studies also showed that the linear range of detection for the Cu^{2+} ions was 0–12 μM (Fig. S5†), while for Hg^{2+} ions, it was 0–18 μM (Fig. S6†). An increase in the effective conjugation was further evidenced from the non-localized distribution of frontier molecular orbitals (FMOs) over the entire molecular framework (Fig. S7†). Monitoring the responses of the probe toward metal ions over a broad pH range (from 4.0 to 9.0) indicated that the efficiency of the probe almost remains unaffected beyond pH 5 (Fig. S8†). The robustness of the present protocol was ensured by monitoring the Cu^{2+} or Hg^{2+} induced change in the presence of an excess of other interfering analytes (Fig. 2a inset). Comparatively lower detection limits of 11 ppb (for Cu^{2+} ion) and 1.15 ppb (for Hg^{2+} ion) were estimated using the blank variation method.[24]

The fluorescence spectra of **1** (λ_{ex} = 355 nm, excitation for phenanthroline unit) mainly consists of a characteristic phenanthroline signature (λ_{max} = 430 nm) with a small peak at 577 nm due to the dynamic equilibrium existing between the non-planar 'closed ring' conformation and highly emissive 'open-ring' xanthene structure. However, the addition of Hg^{2+} selectively induced the appearance of a bright red fluorescence with ~90-fold enhancement in xanthene emission (λ_{max} = 585 nm, ϕ = 0.36) (Fig. 2b). This might be due to the remodeling of the free hanging of a rhodamine analog (in free **1**) into a highly conjugated rigid structure upon coordination with a metal ion, enhancing the extent of energy transfer from phenanthroline to rhodamine unit (Fig. 2). This was also evidenced from the time-dependent emission decay (TCSPC) studies, where the multiexponential long-lived decay profile of the flexible free probe was found to be diminished upon interaction with Hg^{2+} (Fig. S9†).[25] Other metal ions, including Cu^{2+}, did not induce any alteration in the emission spectra of the probe (Fig. 2b inset). Therefore, this differential optical response of **1** towards Hg^{2+} and Cu^{2+} allowed for the detection and discrimination of both metal ions. However, from Fig. 3a, it was quite clear that the alternate addition of Cu^{2+} within the **1** + Hg^{2+} system did not affect the selectivity of **1** towards Hg^{2+}. So, from this response, we can conclude that although **1** was able to detect Cu^{2+} and Hg^{2+} individually, in an ionic mixture, it will selectively isolate and capture Hg^{2+}. Fig. 3b shows the selectivity of **1** towards Hg^{2+} in the individual presence of different cations (1 : 1 situation), and undoubtedly indicated the versatility of **1** towards Hg^{2+} compared to other cations, including Cu^{2+}. Here also, saturation in the optical response was achieved upon the addition of ~2 equiv. of Hg^{2+} ion (Fig. S10†). Finally, from Fig. 3c, it is evident that in an ionic mixture, *i.e.*, in the presence of all the cations in the mixture, **1** was equally efficient to identify, capture and separate Hg^{2+}. These experiments undoubtedly indicated the versatility of **1** towards the selective and sensitive chemosensing of Hg^{2+} in real situations.

Interaction of rhodamine-based sensors with metal ions can occur either through ion-induced spirolactam ring opening or ion catalyzed hydrolysis reaction.[26] The EDTA-mediated recovery experiment with both Hg^{2+} and Cu^{2+} clearly indicated that the observed optical changes were due to the reversible spirolactam ring opening, and not due to ion-induced hydrolysis (Fig. 3b). In both cases, the 1 : 1 stoichiometry of interaction was evaluated from Job's plot analysis (Fig. S11†).[27] The association constants were calculated as 4.69 ± 0.01 (for Hg^{2+}) and 3.97 ± 0.01 (for Cu^{2+}) based on the Benesi–Hildebrand model for 1 : 1 interaction (Fig. S12†).[28] This was further supported from the ESI mass spectra of probes in the presence of the corresponding metal ions, where peaks corresponding to the 1 : 1 metal complex could be observed (Fig. S13†).

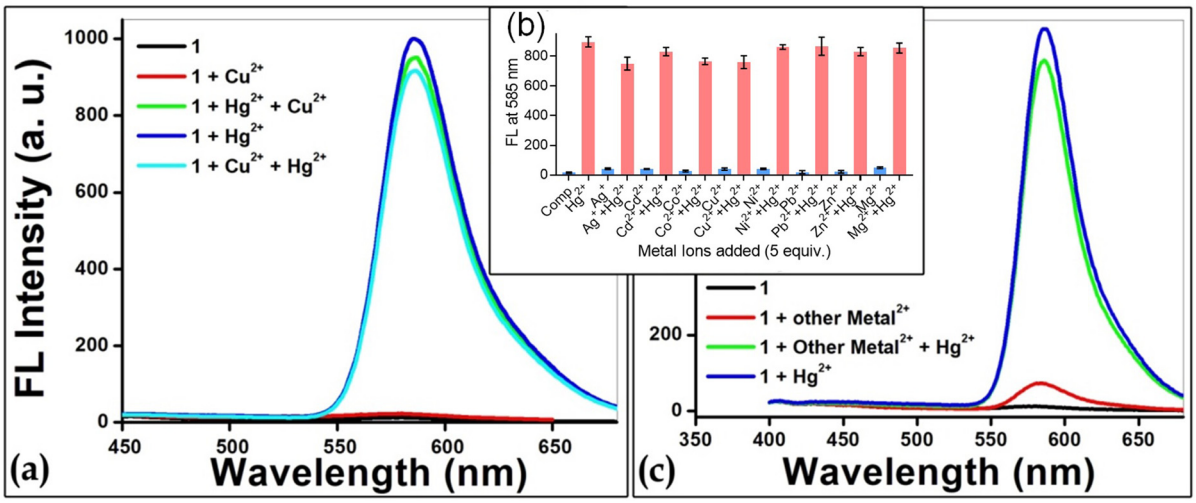

Fig. 3 (a) Response of **1** towards the alternate addition of Hg^{2+} and Cu^{2+} ion (b) in the individual presence of other cations (in excess) monitored at 585 nm. (c) Versatile selectivity plot of **1** towards Hg^{2+} in an ionic mixture.

4.2. Mechanism of metal ion interaction

Now, in order to evaluate the exact binding mode of metal ion recognition (phenanthroline or rhodamine), we have performed ^{1}H NMR titration of **1** upon the gradual addition of both Hg^{2+} and Cu^{2+} in $CDCl_3$. The paramagnetic nature of Cu^{2+} (d^9, open shell configuration) induced quenching of all of the molecular peaks. However, during interaction with Hg^{2+}, the phenanthroline protons (H_a, H_b, and H_c) experienced a greater extent of downfield shift compared to the protons present near the vicinity of the carbonyl group of the rhodamine functionality (Fig. 4). On the other hand, the downfield shift of xanthene protons (with prominent broadening) signified the opening of the spirolactam ring during metal ion coordination. This clearly indicated that the metal ion (here Hg^{2+}) interacted with the probe through the phenanthroline nitrogen ends, rather than the carbonyl group of the spirolactam ring. To further support this, we have recorded the FT-IR spectra of **1** both in the absence and presence of Cu^{2+} and Hg^{2+} ions. The complexation with of either of these ions did not show any visible change in the carbonyl (C═O) stretching frequency, which excluded the involvement of the carbonyl group in the interaction (Fig. S14†).

4.3. Interaction with different anions

Now, *in situ* generated metal complexes have gained immense popularity in recent years due to their highly specific interaction ability towards a wide range of analytes, including toxic anions, phosphates, and amino acids.[29] In this context, Cu^{2+} and Hg^{2+} appeared to be one of the promising templates due to their versatile complexation ability by modifying the coordination sites. The addition of toxic anions like CN^- and I^- to the **1** + Cu^{2+} solution (**1** : Cu^{2+} = 1 : 1) resulted in a vivid color change from bright pink to colorless. The characteristic absorption band of the metal complex at ~560 nm was found to be diminished accordingly (Fig. 5b). Here, we achieved saturations upon the addition of ~2 equiv. of anions (with respect to the Cu^{2+} concentration), which ensured 1 : 2 complexation with the *in situ* generated metal complex in both cases (Fig. S15 and S16†).

However, the interaction of the anions with the *in situ* generated Hg^{2+} complex revealed selective recognition of only CN^- ion (Fig. 5a). Herein, the diminishing of the 562 nm absorption maxima was also reflected from the discoloration of the bright pink colored solution of **1**. No further observed decrease of the absorbance (at 562 nm) beyond ~2 equiv. of CN^- ion addition implied a 1 : 2 interactive model (Fig. S17†). In the emission, a Hg^{2+}-induced 'Turn-On' fluorescence was also found to be quenched (λ_{max} = 585 nm) selectively in the presence of CN^- only (Fig. S18 and S19†). Thus, following the systematic investigations, we could selectively identify both CN^- and I^- ions. The optical responses clearly demonstrated that all these anions interact with probe through metal ion (Cu^{2+} or Hg^{2+}) center. A reversible interaction was established (CN^- and I^-) when the metal ions and anions were added sequentially for multiple times (Fig. S20†). Similarly, the ^{1}H NMR spectra of **1** + Hg^{2+} (1 : 1) showed the regeneration of compound peaks upon the addition of the CN^- ion (Fig. S21†). So, it can be certainly concluded that the interaction of the anions with the metal complex was simply through the displacement of the corresponding metal ion from **1**, rather than the formation of a ternary complex (Fig. 6).

4.4. Fast-track detection of toxic metal ions using paper-discs

The laboratory-developed sophisticated analytical methods often face difficulties in functioning in remote areas due to the lack of trained technicians or advanced instrumental set-ups. Thus, we planned to develop a parallel strategy to build low-cost, portable paper discs for both Cu^{2+} and Hg^{2+} in aqueous medium (which does not require a sophisticated instrument or experienced technicians). The dye-coated paper discs

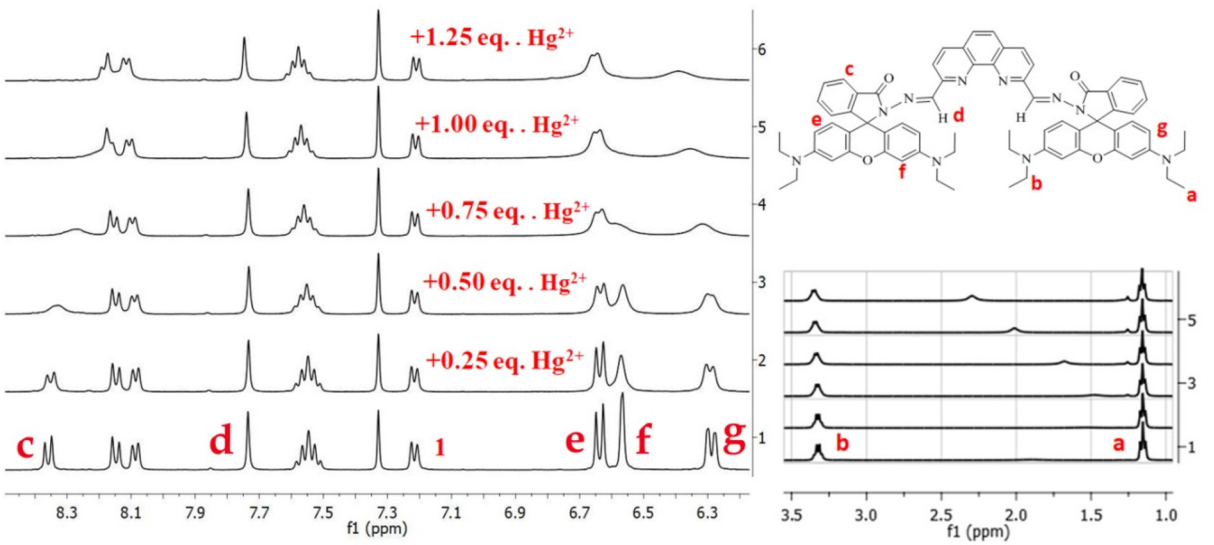

Fig. 4 Partial ^{1}H NMR spectra of **1** upon the gradual addition of Hg^{2+} (0 to 1 equiv. arranged from bottom to top) in $CDCl_3$ medium. The structure of the compound along with the involved protons was shown for convenience.

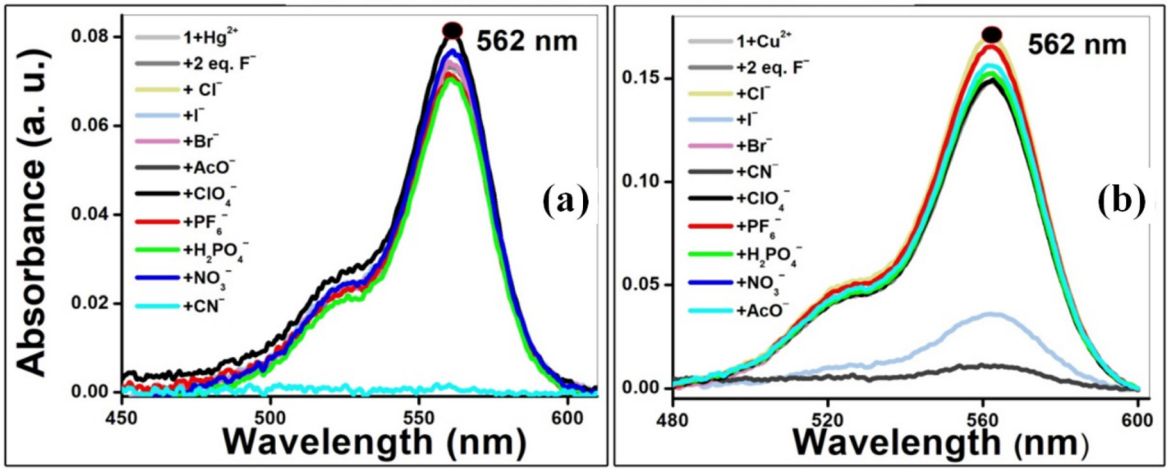

Fig. 5 (a) UV-visible spectra of **1** + Hg^{2+} ([**1**] = 10 μM, **1** : Hg^{2+} = 1 : 1) with different anions in acetonitrile–water (1 : 1) medium. (b) UV-visible spectra of **1** + Cu^{2+} ([**1**] = 10 μM, **1** : Cu^{2+} = 1 : 1) with different anions in acetonitrile–water (1 : 1) medium.

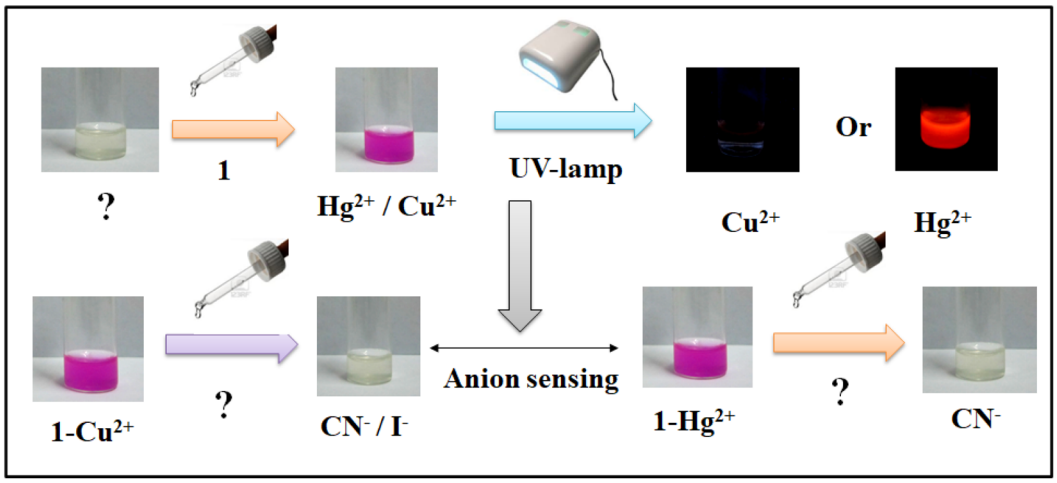

Fig. 6 Schematic diagram showing the simultaneous detection of four different ionic analytes through the single molecular probe **1**.

showed no color to begin with (with no emission under UV lamp). However, addition of both Cu^{2+} and Hg^{2+} induced the formation of a red-color spot almost instantaneously.[30] When the Hg^{2+}-treated disc was kept under long UV lamp, a bright red-colored emission was observed, which was not the case with Cu^{2+}. Thus, the present probe can not only detect these two ions, but can also eventually discriminate between them (Fig. 7b). The addition of other metal ions did not induce any noticeable change in the color or texture of the discs. This certainly established the specific nature of 1 towards the Cu^{2+} and Hg^{2+} ions. The extent of color change in all cases was further quantified using ImageJ software (Fig. S22†).

4.5. Development of molecular logic system

Multiple responses in the absorption and emission spectra of **1** upon the case specific interaction with different cations (Hg^{2+} and Cu^{2+}) and anions (CN^-/I^-) individually, as well as in mixture, were successfully exploited to construct different optical switches. The formation of different simple one input logic gates (NOT and YES) were also able to portray different trivial logic gates (like OR, NOR) and some non-trivial logic gates (such as IMPLICATION, TRANSFER (NOT-TRANSFER), INHIBIT, COMPLEMENT). The most fascinating thing of this existing report is that a single photochemical system could be tuned effortlessly to execute absolutely special binary logic features (like OR to NOR, INHIBIT to IMPLICATION *etc.*) primarily based on the choice of only the optical output channel, while keeping other parameters (primary system, inputs) as is.

4.5.1. Considering the absorption changes of 1 upon interaction with Hg^{2+} and Cu^{2+}. Employing **1** as the primary state alongside two chemical inputs, "Input **Cu^{2+}**" and "Input **Hg^{2+}**" and optical output at several absorption wavelengths, we were able to construct different logic systems (Table 1). As illustrated in Table 1, following different absorption values at 562 nm, a simple OR logic gate was constructed. As reflected from the bar diagram in Fig. 8a, we will get high absorbance

(a)

System	Medium	Linear Response (r^2)	Detection limit (ppb)
With Hg^{2+}	In Tap water	0.975	2.4 ± 0.01
	In Pool water	0.981	3.2 ± 0.02
	In Sea water	0.978	5.6 ± 0.07
With Cu^{2+}	In Tap water	0.962	15.2 ± 0.03
	In Pool water	0.953	16.5 ± 0.03
	In Sea water	0.974	24.7 ± 0.08

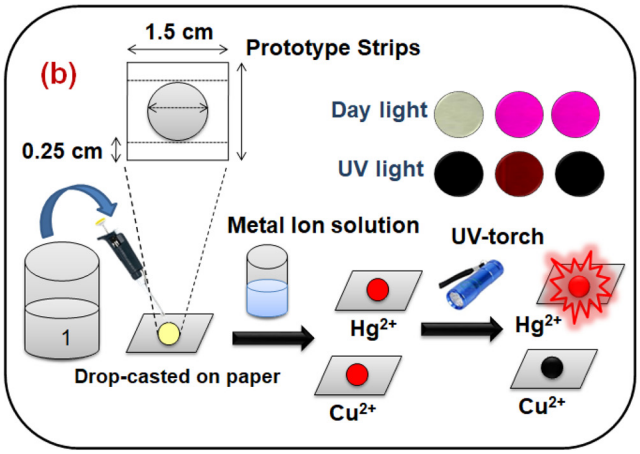

Fig. 7 (a) Detection limit of **1** for Cu^{2+} and Hg^{2+} in different natural water sources. (b) Photographs of the test strips made from **1** (50 μM) for the detection of Cu^{2+} and Hg^{2+} both under daylight and under UV lamp (365 nm).

Table 1 Truth table for binary arithmetic absorption responses received from **1** upon interaction with Hg^{2+} and Cu^{2+}, after application of proper thresholds to the corresponding channel

Cu^{2+}	Hg^{2+}	$A_{562\ nm}$ (OR)	$A_{370\ nm}$ (COMPLEMENT)	$A_{278\ nm}$ (NOR)
0	0	0	1	1
1	0	1	1	0
0	1	1	0	0
1	1	1	0	0

values at 562 nm for the individual ion, as well as simultaneous presence of both ions (Hg^{2+} and Cu^{2+}). We will get low absorption at 562 nm channels (binary 0) only when the pure probe is present. Thus, the opto-chemical response in binary terms perfectly mimicked the OR logic response.

Again, the absorbance values at 370 nm after application of a proper threshold perfectly mimicked the binary logic response of a **COMPLEMENT** logic gate composed of the two AND, one NOT, and NOR gates was portrayed. In this case, we will get the ON state for the pure **1** and **1**-Cu^{2+} systems, *i.e.*, (0,0) and (1,0) input situations. Finally, if we switch the absorbance channel to 278 nm again, we could easily design a **NOR** logic by applying a suitable threshold to the absorbance responses generated at different input situations. Here, we will get the ON state (binary 1) in the absence of any of the chemical inputs (0,0 state). Thus, we can switch the logic response from one to another (**OR** to **COMPLEMENT** to **NOR**) by effortlessly toggling the output channel to (562 to 370 to 278 nm).

4.5.2. Considering the absorption changes of 1 upon interaction with Hg^{2+} and CN^-. Considering **1** as the preliminary state with the subsequent two chemical inputs, "Input **Hg^{2+}**" and "Input **CN^-**", we were able to construct dual-complementary INHIBIT-IMPLICATION logic systems (Table 2) at two different absorption channels. As a primary component for

Table 2 Truth table for binary arithmetic absorption responses received from **1** upon interaction with Hg^{2+} and CN^-, after application of proper thresholds to the corresponding channel

Hg^{2+}	CN^-	$A_{562\ nm}$ (INHIBIT)	$A_{370\ nm}$ (IMPLICATION)
0	0	0	1
1	0	1	0
0	1	0	1
1	1	0	1

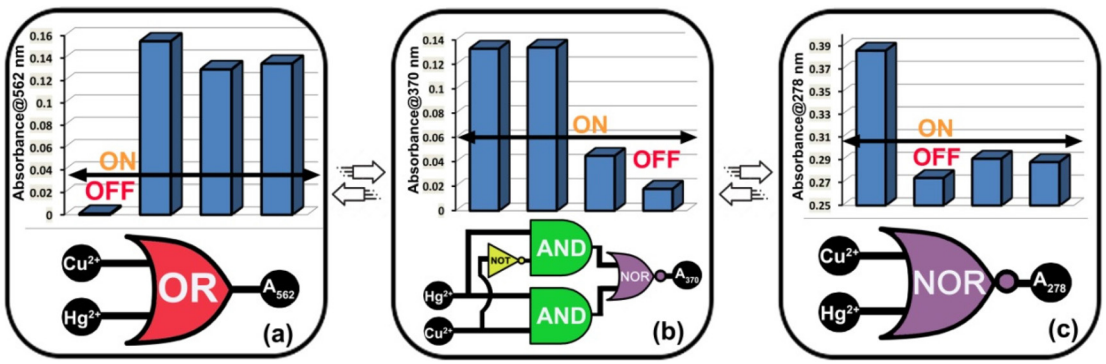

Fig. 8 Optical bar responses and corresponding schematic logic presentation of OR (a), COMPLEMENT (b) and NOR (c) logic gates based on the absorbance responses of **1** at 562, 370 and 278 nm, respectively, considering Hg^{2+} and Cu^{2+} as chemical inputs.

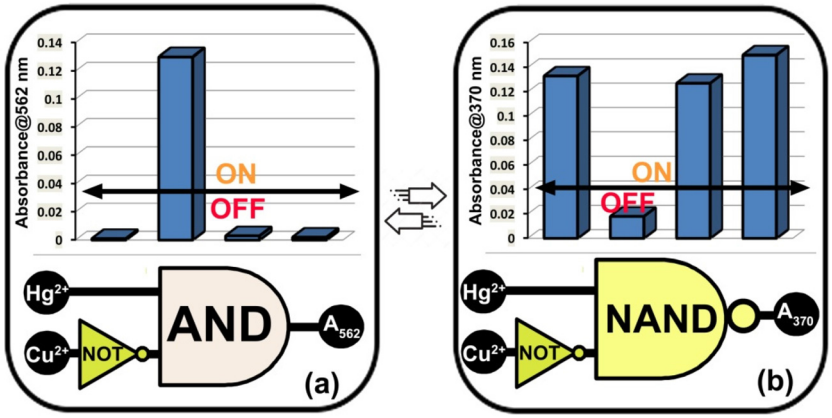

Fig. 9 Optical bar responses and corresponding schematic logic presentation of INHIBIT (a) and IMPLICATION (b) logic gates based on the absorbance responses of **1** at 562 nm and 370 nm, respectively, considering Hg^{2+} and CN^{-} as chemical inputs.

molecular calculators, or "moleculators", (where binary addition and subtraction could be executed on molecule-based systems) INHIBIT logic gate, a combination of individual AND and NOT logic gates recently emerged.[31] As illustrated in Table 2, following different absorption values at 562 nm, an **INHIBIT** logic gate was constructed, where we will get the ON state (binary 1 value) for the (1,0) input situation only (Fig. 9a).

Simultaneously, with the same setup, we will get an **IMPLICATION** logic gate response by simply toggling the absorption channel from 562 nm to 370 nm. The binary response if this gate is completely opposite to that of the INHIBIT gate (Fig. 9b). For scheming numerous logic arrays, such as adder and half adder in combination with the FALSE function, **IMPLICATION** drew special attention.[32]

4.5.3. Considering the absorption changes of 1 upon interaction with Hg^{2+} and I^{-}. Utilizing **1** as the initial system with two chemical inputs, "Input Hg^{2+}" and "Input I^{-}", we were able to design dual-complementary non-trivial **TRANSFER** & **NOT-TRANSFER** logic systems at 562 nm & 370 nm absorption wavelengths (Table 3). As illustrated in Table 3, following different absorption values at 562 nm, a **TRANSFER** logic gate was constructed (Fig. 10a). Transfer gates effortlessly switch

Table 3 Truth table for binary arithmetic absorption responses received from **1** upon interaction with Hg^{2+} and I^{-}, after application of proper thresholds to the corresponding channel

Hg^{2+}	I^{-}	$A_{562\ nm}$ (TRANSFER)	$A_{370\ nm}$ (NOT-TRANSFER)
0	0	0	1
1	0	1	0
0	1	0	1
1	1	1	0

Table 4 Truth table for binary arithmetic fluorescence response received from **1** upon interaction with Cu^{2+} and Hg^{2+}, after application of proper thresholds to the corresponding channel

Cu^{2+}	Hg^{2+}	$FI_{585\ nm}$ (TRANSFER)
0	0	0
1	0	0
0	1	1
1	1	1

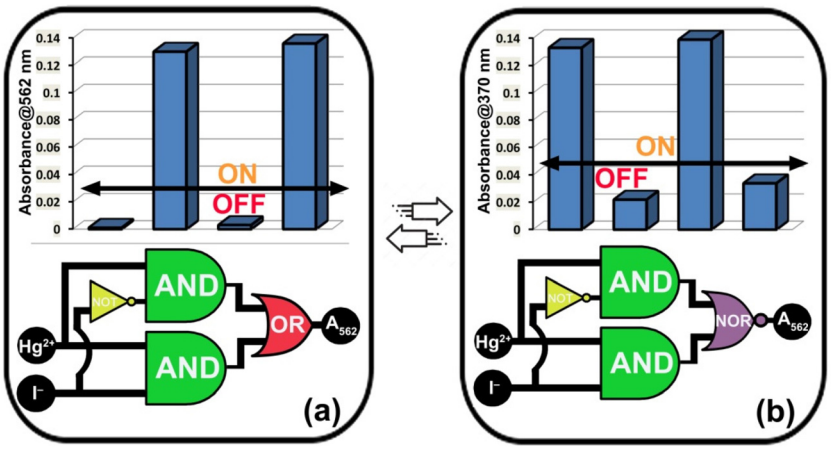

Fig. 10 Optical bar responses and corresponding schematic logic presentation of TRANSFER (a) and NOT-TRANSFER (b) logic gates based on the absorbance responses of **1** at 562 nm and 370 nm, respectively, considering Hg^{2+} and I^{-} as chemical inputs.

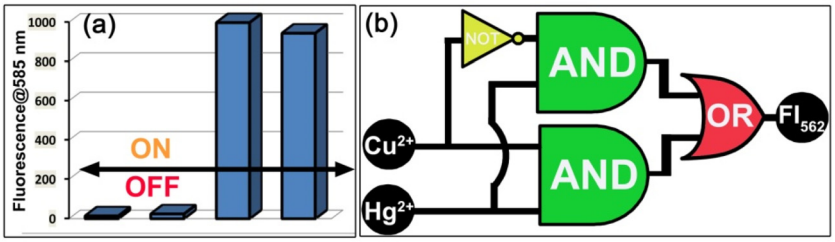

Fig. 11 (a) Optical bar responses and (b) corresponding schematic logic presentation of the **TRANSFER** logic gate based on the fluorescence responses of **1** at 562 nm, considering Cu^{2+} and Hg^{2+} as chemical inputs.

the state of an input to that of an output with no logical trade (0 turns into 0, 1 turns into 1). They are beneficial in structures of concatenated common logic gates for the conversion of the output of one gate into the input of a second. Concatenation of gates is indispensable if a molecular logic system is to be used to perform complex computational operations.[33] As reflected from Table 3, the output response of the system at 562 nm simply mimicked the "Input Hg^{2+}" state in terms of binary values.

Again, considering the absorbance values at 370 nm, a **NOT-TRANSFER** logic gate was portrayed (Fig. 10b). Here, the binary logic values are completely opposite to that of the proposed TRANSFER logic gate response at 562 nm. Thus, one can simply switch from **TRANSFER** to **NOT-TRANSFER** and *vice versa* logic response by simply switching the output channel from 562 nm to 370 nm and *vice versa*.

Additionally, employing **1** as device with two chemical inputs, "Input **Cu^{2+}**" and "Input **CN^-/I^-**" and optical output at several absorption wavelengths, we were able to construct different logic systems (Table S1†). As illustrated in Table S1,† following different absorption values at 562 nm, an **INHIBIT** logic gate was constructed (Fig. S23†).

4.5.4. Considering the emission changes of 1 upon interaction with Hg^{2+} and Cu^{2+}. Finally, employing **1** as a device with two chemical inputs, "Input **Cu^{2+}**" and "Input **Hg^{2+}**", and optical output at several emission wavelengths, we were able to construct different logic systems (Table 4). As illustrated in Table 4, following different absorption values at 562 nm, a **TRANSFER** logic gate was constructed (Fig. 11).

In fluorescence studies, we will get a Turn ON response only in the presence of Input Hg^{2+}, *i.e.*, in binary terms "1" value. For the rest of the situations, as we did not get any fluorescence response, the output responses were also "0". This **TRANSFER** logic response is quite different from the above-mentioned one (Fig. 11).

5. Conclusions

In conclusion, we have developed an easily synthesizable chromophoric probe comprising the metal ion sensitive phenanthroline and rhodamine moiety through the connection of an imine bond. Interaction of the compound with Hg^{2+} or Cu^{2+} triggered the emergence of a bright pink color in a semi-aqueous environment. However, in emission mode, only Hg^{2+} induced a 'Turn-On' response. However, fluorescence selectivity studies revealed that Probe **1** was quite versatile to exclusively identify and capture Hg^{2+} ion in an ionic mixture, even in the presence of Cu^{2+} in the ionic mixture. Furthermore, these *in situ* generated metal complexes were employed for the detection of different toxic anions. Selective recognition of both CN^- and I^- ions were achieved through the displacement of the corresponding metal ions from the vicinity of the probe. Thus, by utilizing a single probe, we had established **1** as a versatile 'naked-eye' Hg^{2+} sensor with ppb level sensing efficiency. We also achieved the ppb level 'naked-eye' detection of four different analytes: Cu^{2+}, Hg^{2+}, CN^- and I^- individually. Furthermore, the detection of metal ions was achieved in different natural water sources, and also using paper-discs. Ultimately, on a single molecular probe **1** based totally on differential opto-chemical interactions with special ions (Cu^{2+}, Hg^{2+}, CN^- and I^-), we are able to diagram several trivial (OR, NOR) as well as non-trivial (INHIBIT, IMPLICATION, COMPLEMENT, TRANSFER, NOT-TRANSFER) logic gates. Most fascinatingly, we can swap the logic response from one kind to another *via* easy tuning of only the optical output channel.

Conflicts of interest

The authors declare no conflict of interest.

Acknowledgements

The author N. D. thanks BITS Pilani Hyderabad for additional competitive research grant (ACRG), and also central analytical facilities for all technical support. R. S. F. thanks BITS Pilani, Hyderabad for a research fellowship.

References

1 E. L. Que, D. W. Domaille and C. J. Chang, Metals in Neurobiology: Probing Their Chemistry and Biology with Molecular Imaging, *Chem. Rev.*, 2008, **108**, 1517.
2 (*a*) E. S. Forzani, H. Zhang, W. Chen and N. Tao, Detection of Heavy Metal Ions in Drinking Water Using a High-

Resolution Differential Surface Plasmon Resonance Sensor, *Environ. Sci. Technol.*, 2005, **39**, 1257; (*b*) E. L. Frank, M. P. Hughes, D. D. Bankson and W. L. Roberts, Effects of anticoagulants and contemporary blood collection containers on aluminum, copper, and zinc results, *Clin. Chem.*, 2001, **47**, 1109.

3 B. Vennesland, E. E. Comm, C. J. Knownles, J. Westly and F. Wissing, *Cyanide in Biology*, Academic Press, London, 1981.

4 (*a*) L. Chen, W. Lu, X. Wang and L. Chen, A highly selective and sensitive colorimetric sensor for iodide detection based on anti-aggregation of gold nanoparticles, *Sens. Actuators, B*, 2013, **182**, 482; (*b*) Y. Wang, H. Zhu, X. Yang, Y. Dou and Z. Liu, New colorimetric and fluorometric sensing strategy based on the anisotropic growth of histidine-mediated synthesis of gold nanoclusters for iodide-specific detection, *Analyst*, 2013, **138**, 2085.

5 (*a*) N. Boens, V. Leen and W. Dehaen, Fluorescent indicators based on BODIPY, *Chem. Soc. Rev.*, 2012, **41**, 1130; (*b*) L. Yuan, W. Lin, K. Zheng, L. He and W. Huang, Far-red to near infrared analyte-responsive fluorescent probes based on organic fluorophore platforms for fluorescence imaging, *Chem. Soc. Rev.*, 2013, **42**, 622.

6 (*a*) V. Dujols, F. Ford and A. W. Czarnik, A long-wavelength fluorescent chemodosimeter selective for Cu(II) ion in water, *J. Am. Chem. Soc.*, 1997, **119**, 7386; (*b*) L. M. Hyman and K. J. Franz, Probing oxidative stress: Small molecule fluorescent sensors of metal ions, reactive oxygen species, and thiols, *Coord. Chem. Rev.*, 1997, **256**, 2333; (*c*) X. Chen, T. Pradhan, F. Wang, J. S. Kim and J. Yoon, Fluorescent Chemosensors Based on Spiroring-Opening of Xanthenes and Related Derivatives, *J. Chem. Rev.*, 2012, **112**, 1910 and references therein; (*d*) H. N. Kim, M. H. Lee, H. J. Kim, J. S. Kim and J. Yoon, A new trend in rhodamine-based chemosensors: application of spirolactam ring-opening to sensing ions, *Chem. Soc. Rev.*, 2008, **37**, 1465 and references therein.

7 (*a*) Y. Leng, S. Qian, Y. Wang, C. Lu, X. Ji, Z. Lu and H. Lin, Single-indicator-based Multidimensional Sensing: Detection and Identification of Heavy Metal Ions and Understanding the Foundations from Experiment to Simulation, *Sci. Rep.*, 2016, **5**, 25354; (*b*) M. Chhatwal, A. Kumar, V. Singh, R. D. Gupta and S. K. Awasthi, Addressing of multiple-metal ions on a single platform, *Coord. Chem. Rev.*, 2015, **292**, 30; (*c*) Y. W. Choi, G. J. Park, Y. J. Na, H. Y. Jo, S. A. Lee, G. R. You and C. Kim, A single schiff base molecule for recognizing multiple metal ions: a fluorescence sensor for Zn(II) and Al(III) and colorimetric sensor for Fe(II) and Fe(III), *Sens. Actuators, B*, 2014, **194**, 343; (*d*) B. Rout, A Miniaturized Therapeutic Chromophore for Multiple Metal Pollutant Sensing, Pathological Metal Diagnosis and Logical Computing, *Sci. Rep.*, 2016, **6**, 27115; (*e*) V. V. Kumar, M. K. Thenmozhi, A. Ganesan, S. S. Ganesan and S. P. Anthony, Hyperbranched polyethylenimine-based sensor of multiple metal ions (Cu^{2+}, Co^{2+} and Fe^{2+}): colorimetric sensing via coordination or AgNP formation, *RSC Adv.*, 2015, **5**, 88125; (*f*) B. Tao, N. Wu, H. Zhang and H. Wang, Blocking the Cu(II) Ions Mediated Catalytical Ability for Construction of Ratiometric Fluorescence Sensing Platform Based on Glutathione-Stabilized Copper Nanoclusters, *J. Electrochem. Soc.*, 2022, **169**, 037529; (*g*) H. Wang, A. Mao, B. Tao, H. Zhang and Y. Liu, Fabrication of multiple molecular logic gates made of fluorescent DNA-templated Au nanoclusters, *New J. Chem.*, 2021, **45**, 4195; (*h*) H. Wang, H. Bai, Y. Wang, T. Gan and Y. Liu, Highly selective fluorimetric and colorimetric sensing of mercury(II) by exploiting the self-assembly-induced emission of 4-chlorothiophenol capped copper nanoclusters, *Microchim. Acta*, 2020, **187**, 185; (*i*) H. Wang, H. Bai, A. Mao, T. Gan and Y. Liu, Poly(adenine)-templated fluorescent Au nanoclusters for the rapid and sensitive detection of melamine, *Spectrochim. Acta, Part A*, 2019, **219**, 375.

8 (*a*) S. Nadella, J. Sahoo, P. S. Subramanian, A. Sahu, S. Mishra and M. Albrecht, Sensing of Phosphates by Using Luminescent Eu^{III} and Tb^{III} Complexes: Application to the Microalgal Cell Chlorella vulgaris, *Chem. – Eur. J.*, 2014, **20**, 6047; (*b*) M. Lee, S. Jo, D. Lee, Z. Xu and J. Yoon, A new naphthalimide derivative as a selective fluorescent and colorimetric sensor for fluoride, cyanide and CO2, *Dyes Pigm.*, 2015, **120**, 288; (*c*) D. Maity, S. Das, S. Mardanya and S. Baitalik, Synthesis, Structural Characterization, and Photophysical, Spectroelectrochemical, and Anion-Sensing Studies of Heteroleptic Ruthenium(II) Complexes Derived from 4′-Polyaromatic-Substituted Terpyridine Derivatives and 2,6-Bis(benzimidazol-2-yl)pyridine, *Inorg. Chem.*, 2013, **52**, 6820; (*d*) A. K. Mahapatra, S. K. Manna, B. Pramanik, K. Maiti, S. Mondal, S. S. Ali and D. Mandal, Colorimetric and ratiometric fluorescent chemodosimeter for selective sensing of fluoride and cyanide ions: tuning selectivity in proton transfer and C–Si bond cleavage, *RSC Adv.*, 2015, **5**, 10716; (*e*) V. K. Gupta, A. K. Singh and N. Gupta, Colorimetric sensor for cyanide and acetate ion using novel biologically active hydrazones, *Sens. Actuators, B*, 2014, **204**, 125; (*f*) E. Saikia, M. P. Borpuzari, B. Chetia and R. Kar, Experimental and theoretical study of urea and thiourea based new colorimetric chemosensor for fluoride and acetate ions, *Spectrochim. Acta, Part A*, 2016, **152**, 101; (*g*) S. Bhattacharjee and S. Bhattacharya, Pyridylenevinylene based Cu^{2+}-specific, injectable metallo (hydro)gel: thixotropy and nanoscale metal–organic particles, *Chem. Commun.*, 2014, **50**, 11690; (*h*) A. D. Tiwari, A. K. Mishra, S. B. Mishra, B. B. Mamba, B. Maji and S. Bhattacharya, Synthesis and DNA binding studies of Ni (II), Co(II), Cu(II) and Zn(II) metal complexes of N1,N5-bis [pyridine-2-methylene]-thiocarbohydrazone Schiff-base ligand, *Spectrochim. Acta, Part A*, 2011, **79**, 1050; (*i*) S. Bhattacharya and M. Thomas, Synthesis of a novel thiazole based dipeptide chemosensor for Cu(II) in water, *Tetrahedron Lett.*, 2000, **41**, 10313; (*j*) S. Bhattacharya and S. S. Mandal, Ambient oxygen activating water soluble cobalt–salen complex for DNA cleavage, *J. Chem. Soc.,*

Chem. Commun., 1995, 2489; (*k*) S. Bhattacharya, K. Snehalatha and S. K. George, Synthesis of Some Copper (II)-Chelating (Dialkylamino)pyridine Amphiphiles and Evaluation of Their Esterolytic Capacities in Cationic Micellar Media, *J. Org. Chem.*, 1998, **63**, 27.

9 (*a*) R. W. Wagner, J. S. Lindsay, J. Seth, V. Palaniappan and D. F. Bocian, Molecular Optoelectronic Gates, *J. Am. Chem. Soc.*, 1996, **118**, 3996; (*b*) N. Tamai, T. Saika, T. Shimidzu and M. Irie, Femtosecond Dynamics of a Thiophene Oligomer with a Photoswitch by Transient Absorption Spectroscopy, *J. Phys. Chem.*, 1996, **100**, 4689; (*c*) P. R. Ashton, V. Balzani, J. Becher, A. Credi, M. C. T. Fyfe, G. Mattersteig, S. Menzer, M. B. Nielsen, F. M. Raymo, J. F. Stoddart, M. Venturi and D. J. Williams, A three-pole supramolecular switch, *J. Am. Chem. Soc.*, 1999, **121**, 3951; (*d*) P. L. Boulas, M. Gomez-Kaifer and L. Echegoyen, Electrochemistry of supramolecular systems, *Angew. Chem., Int. Ed.*, 1998, **37**, 216.

10 (*a*) W. B. Davis, W. A. Svec, M. A. Ratner and M. R. Wasielewski, Molecular-wire behaviour in p-phenylenevinylene oligomers, *Nature*, 1998, **396**, 60; (*b*) B. Schlicke, P. Belser, L. De Cola, E. Sabbioni and V. Balzani, Photonic Wires of Nanometric Dimensions. Electronic Energy Transfer in Rigid Rodlike $Ru(bpy)_3^{2+}$-$(ph)_n$-$Os(bpy)_3^{2+}$ Compounds (ph = 1,4-Phenylene; n = 3, 5, 7), *J. Am. Chem. Soc.*, 1999, **121**, 4207; (*c*) V. Grosshenny, A. Harriman and R. Ziessel, Towards the Development of Molecular Wires: Electron Localization, Exchange, and Transfer in Alkyne–Bridged Multinuclear Complexes, *Angew. Chem., Int. Ed. Engl.*, 1996, **34**, 2705.

11 A. P. de Silva, H. Q. N. Gunaratne, T. A. Gunnlaugsson, J. M. Huxley, C. P. McCoy, J. T. Rademacher and T. E. Rice, Signaling Recognition Events with Fluorescent Sensors and Switches, *Chem. Rev.*, 1997, **97**, 1515.

12 D. Gosztola, M. P. Niemczyk and M. R. Wasielewski, Picosecond Molecular Switch Based on Bidirectional Inhibition of Photoinduced Electron Transfer Using Photogenerated Electric Fields, *J. Am. Chem. Soc.*, 1998, **120**, 5118.

13 A. P. de silva, H. Q. N. Gunaratne and C. P. McCoy, A molecular photoionic AND gate based on fluorescent signalling, *Nature*, 1993, **364**, 42.

14 J. Andréasson and U. Pischel, Molecules with a sense of logic: a progress report, *Chem. Soc. Rev.*, 2015, **44**, 1053.

15 B. Daly, J. Ling and A. P. de Silva, Current developments in fluorescent PET (photoinduced electron transfer) sensors and switches, *Chem. Soc. Rev.*, 2015, **44**, 4203.

16 M. Karar, P. Paul, B. Biswas, A. Mallick and T. Majumdar, Excitation wavelength as logic operator, *J. Chem. Phys.*, 2020, **152**, 075102.

17 M. Suresh, D. A. Jose and A. Das, [2,2′-Bipyridyl]-3,3′-diol as a molecular half-subtractor, *Org. Lett.*, 2007, **9**, 441.

18 A. Coskun, E. Deniz and E. U. Akkaya, Effective PET and ICT Switching of Boradiazaindacene Emission: A Unimolecular, Emission-Mode, Molecular Half-Subtractor with Reconfigurable Logic Gates, *Org. Lett.*, 2005, **7**, 5187.

19 S. J. Langford and T. Yann, Molecular Logic: A Half-Subtractor Based on Tetraphenylporphyrin, *J. Am. Chem. Soc.*, 2003, **125**, 11198.

20 J. Andreasson, S. D. Straight, S. Bandyopadhyay, R. H. Mitchell, T. A. Moore, A. L. Moore and D. Gust, Molecular 2 : 1 Digital Multiplexer, *Angew. Chem., Int. Ed.*, 2007, **46**, 958.

21 S. Erbas-Cakmak, O. A. Bozdemir, Y. Cakmak and E. U. Akkaya, Proof of principle for a molecular 1:2 demultiplexer to function as an autonomously switching theranostic device, *Chem. Sci.*, 2013, **4**, 858.

22 S. Xu, Y.-X. Hao, W. Sun, C.-J. Fang, X. Lu, M.-N. Li, M. Zhao, S.-Q. Peng and C.-H. Yan, 2 : 1 Multiplexing Function in a Simple Molecular System, *Sensors*, 2012, **12**, 4421.

23 (*a*) S. K. Samanta, N. Dey, N. Kumari, D. Biswakarma and S. Bhattacharya, Multimodal Ion Sensing by Structurally Simple Pyridine-End Oligo p-Phenylenevinylenes for Sustainable Detection of Toxic Industrial Waste, *ACS Sustainable Chem. Eng.*, 2019, **7**, 12304; (*b*) N. Dey and S. Bhattacharya, Mimicking multivalent protein–carbohydrate interactions for monitoring the glucosamine level in biological fluids and pharmaceutical tablets, *Chem. Commun.*, 2017, **53**, 5392.

24 E. Ballesteros, D. Moreno, T. Gomez, T. Rodrıguez, J. Rojo, M. Garcıa-Valverde and T. Torroba, A New Selective Chromogenic and Turn-On Fluorogenic Probe for Copper (II) in Water–Acetonitrile 1 : 1 Solution, *Org. Lett.*, 2009, **11**, 1269.

25 S. Lohar, A. Banerjee, A. Sahana, A. Banik, S. K. Mukhopadhyay and D. Das, A rhodamine–naphthalene conjugate as a FRET based sensor for Cr^{3+} and Fe^{3+} with cell staining application, *Anal. Methods*, 2013, **5**, 442.

26 (*a*) N. Dey and S. Bhattacharya, Switchable Optical Probes for Simultaneous Targeting of Multiple Anions, *Chem. – Asian J.*, 2020, **15**, 1759; (*b*) N. Dey, N. Kumari, D. Bhagat and S. Bhattacharya, Smart optical probe for 'equipment-free' detection of oxalate in biological fluids and plant-derived food items, *Tetrahedron*, 2018, **74**, 4457; (*c*) R. S. Fernandes and N. Dey, Ion-specific bathochromic shifts: Simultaneous detection of multiple heavy metal pollutants via charge transfer interactions, *J. Mol. Liq.*, 2022, **367**, 120369; (*d*) R. S. Fernandes and N. Dey, Synthetic Supramolecular Host for D-(−)-Ribose: Ratiometric Fluorescence Response via Multivalent Lectin-Carbohydrate Interactions, *ChemBioChem*, 2022, **23**, e202200044.

27 P. Job, Formation and Stability of Inorganic Complexes in Solution, *Ann. Chim.*, 1928, **9**, 113.

28 H. A. Benesi and B. H. Hildebrand, A Spectrophotometric Investigation of the Interaction of Iodine with Aromatic Hydrocarbons, *J. Am. Chem. Soc.*, 1949, **71**, 2703.

29 (*a*) C. Kaewtong, J. Noiseephum, Y. Uppa, N. Morakot, N. Morakot, B. Wanno, T. Tuntulani and B. Pulpoka, A reversible Em-FRET rhodamine-based chemosensor for carboxylate anions using a ditopic receptor strategy, *New J.*

Chem., 2010, **34**, 1104; (*b*) X. Hu, J. Wang, X. Zhu, D. Dong, X. Zhang, S. Wu and C. Duan, A copper(II) rhodamine complex with a tripodal ligand as a highly selective fluorescence imaging agent for nitric oxide, *Chem. Commun.*, 2011, **47**, 11507; (*c*) X. Lou, D. Ou, Q. Li and Z. Li, An indirect approach for anion detection: the displacement strategy and its application, *Chem. Commun.*, 2012, **48**, 8462.

30 (*a*) S. Paul, R. S. Fernandes and N. Dey, Ppb-level, dual channel sensing of cyanide and bisulfate ions in an aqueous medium: computational rationalization of the ion-dependent ICT mechanism, *New J. Chem.*, 2022, **46**, 18973; (*b*) B. Chettri, S. Jha and N. Dey, Tuning anion binding properties of Bis(indolyl)methane Receptors: Effect of substitutions on optical responses, *Spectrochim. Acta, Part A*, 2023, **287**, 121979; (*c*) S. Jha, N. Kumari, B. Chettri and N. Dey, Monitoring Local pH of Membranous Aggregates via Ratiometric Color Changing Response, *ChemPhysChem*, 2022, **23**, e202200208; (*d*) D. Sunil, K. Muthamma, S. D. Kulkarni, R. S. Fernandes and N. Dey, Barbituric acid derivative as fluorescent pigment in water-based flexographic ink for security applications, *Chem. Pap.*, 2023, **77**, 119–127.

31 (*a*) U. Pischel, Chemical approaches to molecular logic elements for addition and subtraction, *Angew. Chem., Int. Ed.*, 2007, **46**, 4026; (*b*) D. Margulies, G. Melman and A. Shanzer, Fluorescein as a model molecular calculator with reset capability, *Nat. Mater.*, 2005, **4**, 768.

32 M. Elstner, J. Axthelm and Al. Schiller, Sugar-based Molecular Computing by Material Implication, *Angew. Chem., Int. Ed.*, 2014, **53**, 7339.

33 (*a*) T. Gupta and M. E. van der Boom, Redox-Active Monolayers as a Versatile Platform for Integrating Boolean Logic Gates, *Angew. Chem., Int. Ed.*, 2008, **47**, 5322; (*b*) G. Seelig, D. Soloveichik, D. Y. Zhang and E. Winfree, Enzyme-Free Nucleic Acid Logic Circuits, *Science*, 2006, **314**, 1585; (*c*) B. M. Frezza, S. L. Cockroft and M. R. Ghadiri, Modular Multi-Level Circuits from Immobilized DNA-Based Logic Gates, *J. Am. Chem. Soc.*, 2007, **129**, 14875.

